arXiv:1606.06862v2 [astro-ph.GA] 11 Jul 2016

VARIABLE STARS AND STELLAR POPULATIONS IN ANDROMEDA XXV: III. A CENTRAL CLUSTER OR THE GALAXY NUCLEUS? *

FELICE CUSANO[1], ALESSIA GAROFALO[1,2], GISELLA CLEMENTINI[1], MICHELE CIGNONI[3], LUCIANA FEDERICI[1], MARCELLA MARCONI[4], VINCENZO RIPEPI[4], ILARIA MUSELLA[4], VINCENZO TESTA[5], ROBERTA CARINI[5], MARCO FACCINI[5]

[1] *INAF- Osservatorio Astronomico di Bologna, Via Ranzani 1, I - 40127 Bologna, Italy*

felice.cusano@oabo.inaf.it

[2] *Dipartimento di Fisica e Astronomia, Università di Bologna, viale Berti Pichat, 6/2, I - 40127 Bologna, Italy*

[3] *Dipartimento di Fisica, Università di Pisa, Largo Bruno Pontecorvo, 3, 56127 Pisa PI*

[4] *INAF- Osservatorio Astronomico di Capodimonte, Salita Moiariello 16, I - 80131 Napoli, Italy*

[5] *INAF- Osservatorio Astronomico di Roma, Via di Frascati 33 00040 Monte Porzio Catone, Italy*

ABSTRACT

We present B and V time-series photometry of Andromeda XXV, the third galaxy in our program on the Andromeda's satellites, that we have imaged with the Large Binocular Cameras of the Large Binocular Telescope. The field of Andromeda XXV is found to contain 63 variable stars, for which we present light curves and characteristics of the light variation (period, amplitudes, variability type, mean magnitudes, etc.). The sample includes 58 RR Lyrae variables (46 fundamental-mode − RRab, and 12 first-overtone −RRc, pulsators), three anomalous Cepheids, one eclipsing binary system and one unclassified variable. The average period of the RRab stars ($\langle Pab \rangle = 0.60$ $\sigma = 0.04$ days) and the period-amplitude diagram place Andromeda XXV in the class of the Oosterhoff-Intermediate objects. From the average luminosity of the RR Lyrae stars we derive for the galaxy a distance modulus of (m-M)$_0$=24.63 ± 0.17 mag. The color-magnitude diagram reveals the presence in Andromeda XXV of a single, metal-poor ([Fe/H]=−1.8 dex) stellar population as old as $\sim$ 10-12 Gyr traced by a conspicuous red giant branch and the large population of RR Lyrae stars. We discovered a spherically-shaped high density of stars near the galaxy center. This structure appears to be at a distance consistent with Andromeda XXV and we suggest it could either be a star cluster or the nucleus of Andromeda XXV. We provide a summary and compare number and characteristics of the pulsating stars in the M31 satellites analyzed so far for variability.

Subject headings: galaxies: dwarf, Local Group —galaxies: individual (Andromeda XXV) —stars: distances —stars: variables: general —techniques: photometric

1. INTRODUCTION

In the framework of the Λ Cold Dark Matter (ΛCDM) theory, large galaxies like Andromeda

* Based on data collected with the Large Binocular Cameras at the Large Binocular Telescope

(M31) are formed through accretion and merging of smaller structures (e.g. Bullock & Johnston 2005). The satellites that we observe today around M31 could be the surviving left-overs of the galaxy hierarchical accretion process. Their stellar contents can thus provide important hints to reconstruct the star formation history and the merging episode that led to the formation of M31. The analysis of the color-magnitude diagram (CMD) represents the most powerful tool for such investigations. However, given the distance of the M31 complex, ground-based observations barely reach the bottom of the red giant branch (RGB) of these satellite galaxies and can extend down to the horizontal-branch (HB) only when 8-10 m class telescopes are used. For this reason pulsating variable stars such as the RR Lyrae stars, which populate the HB of an old ($t \gtrsim 10$ Gyr) stellar population, and the brighter and younger Cepheids, are powerful alternative tools to trace and characterize the different stellar generations in these systems.

This is the third paper in our series on the M31 satellites based on B and V time-series photometry obtained with the Large Binocular Cameras (LBC) of the Large Binocular Telescope (LBT). We characterize the resolved stellar populations of the M31 companions using the CMD and the properties of variable stars and from this derive hints on the nature, origin and fate of Andromeda's satellites in the global context of merging and accretion episodes occurring in M31. Details on the survey and results from the study of Andromeda XIX (And XIX) and Andromeda XXI (And XXI) were presented in Cusano et al. (2013, Paper I) and Cusano et al. (2015, Paper II), respectively. In this paper we report results on Andromeda XXV (And XXV).

And XXV was discovered by Richardson et al. (2011) in the context of the PAndAS survey (Martin et al. 2013, and reference therein) and later found to be a member of the thin plane of satellites identified in M31 by Ibata et al. (2013). The discovery paper reports a distance modulus of (m-M)$_0$= 24.55 $\pm$ 0.12 mag for And XXV from the luminosity of the galaxy HB and a half-light radius (r$_h$) of 3.0$'$ (corresponding to $r_h = 732 \pm 60$ pc at the distance of And XXV). Later, Conn et al. (2012), adopting a bayesian approach to locate the tip of the red giant branch, have revised the distance modulus of And XXV to (m-M)$_0$= $24.33^{+0.07}_{-0.21}$ mag. This is more than 1 σ shorter than Richardson et al. (2011)'s distance based on the HB luminosity. And XXV has a metallicity of [Fe/H]=-1.9 ± 0.1 dex (Collins et al. 2013) as estimated from the Calcium triplet (CaII) of the galaxy red giants. The same authors measured a velocity dispersion of $\sigma = 3.0^{+1.2}_{-1.1}$ kms^{-1} from 25 spectroscopically confirmed members. This value is rather low, when compared with the large extension of And XXV. Collins et al. (2013) also estimate a mass-to-light ratio inside one r$_h$ of $[M/L]_{r_h} = 10.3\ M_\odot/L_\odot$ that, according to the authors, is consistent with a stellar population without a dark matter component. In a more recent paper Collins et al. (2014) using as an argument the circular velocity within the galaxy half-light radius concluded that the mass of And XXV should have been much more prominent in the past, for the galaxy to be able to form stars. On the other hand, the low velocity dispersion of And XXV's member stars would naturally arise in the context of the MOND theory (McGaugh & Milgrom 2013).

The paper is organized as follows: observations, data reduction and calibration of And XXV photometry are presented in Section 2. Results on the identification and characterization of the variable stars, the catalog of light curves and the Oosterhoff classification of And XXV are discussed in Section 3. The distance to And XXV derived from the RR Lyrae stars is presented in Section 4. The galaxy CMD along with the spatial distribution of the various stellar components are discussed in Section 5. Section 6 examines the discovery of a spherically-shaped high density of stars close to the galaxy center. Main results of the present study are summarized in Section 7.

2. OBSERVATIONS AND DATA REDUCTION

A total of 85 B and 87 V images each of 400 s exposure were obtained with the LBC of a region of $23' \times 23'$ centered on And XXV (R.A.=$00^h30^m08.9^s$, decl. =$+46°51'07''$, J2000.0; Richardson et al. 2011) from the 18th to the 24th of October 2011. Observations in the B band were acquired with the Blue camera and simultaneous

Table 1: Log of And XXV observations

Dates	Filter	N	Exposure time (s)	Seeing (FWHM) (arcsec)
October 18, 2011	B	1	400	1
October 20-24, 2011	B	84	400	0.8-1
October 18, 2011	V	3	400	1
October 20-24, 2011	V	84	400	0.8-1

V imaging with the Red camera of the LBC. All images were obtained under favorable conditions of seeing $\leq 1''$. The log of the observations of And XXV is provided in Table 1.

Photometric reduction of And XXV imaging was carried out following the same procedure as described in detail in Paper I (And XIX) and II (And XXI). The PSF photometry was performed using the `DAOPHOT - ALLSTAR - ALLFRAME` packages (Stetson 1987, 1994). The Landolt standard fields L92 and SA113, observed during the run, were used to derive calibration equations and tie the `DAOPHOT` magnitudes to the Johnson standard system. The new calibration equations[1] are totally consistent with those derived in Paper I, once differences in air-mass and exposure times are accounted for.

3. VARIABLE STARS

The search for variable stars was carried out starting from the variability index computed in `DAOMASTER` (Stetson 1994). The candidate variables were then analyzed by studying their B- and V-band light curves with the Graphical Analyzer of Time Series (GRATIS), private software developed at the Bologna Observatory by P. Montegriffo (see, e.g., Clementini et al. 2000). More details on this procedure can be found in Paper I. We identified, in the B, V datasets of And XXV a total of 63 variable stars: 58 RR Lyrae stars (see Section 3.1), 3 anomalous Cepheids (AC; see Section 3.2), 1 eclipsing binary (ECL) and 1 unclassified variable. The properties of the confirmed variable stars in And XXV are summarized in Table 2. We ordered the variables with an increasing number based on the proximity to the galaxy center, adopting the coordinates by Richardson et al. (2011). Column 1 lists the star identifier, Columns 2 and 3 give the right ascension and declination (J2000 epoch), respectively, obtained from our astrometrized catalogs. Column 4 provides the type of variability. A question mark identifies stars whose classification is uncertain. Columns 5 and 6 list the period and the Heliocentric Julian Day of maximum light, respectively. Columns 7 and 8 give the intensity-weighted mean B and V magnitudes, while Columns 9 and 10 list the corresponding amplitudes of the light variation. The two solid lines in the table separate the variable stars within the area enclosed once and twice the galaxy r_h. Example light curves for RR Lyrae and other types of variables in And XXV are shown in Figure 1. The full catalog of light curves is available in the electronic version only.

3.1. RR LYRAE STARS

In the field of And XXV we have identified a total of 58 RR Lyrae stars: 46 fundamental mode (RRab) and 12 first-overtone (RRc) stars. Fifty-seven of them likely belong to And XXV, whereas V63 is ~ 12 arcmin away from the center of the galaxy and is most probably an RR Lyrae of the M31 halo. We do not include this star when deriving properties of And XXV such as the distance, the Oosterhoff type, etc. Figure 2 shows the period distribution of the RR Lyrae stars. The average period of the whole sample of 45 RRab stars in And XXV is $\langle P_{ab} \rangle$=0.61 d (σ=0.05 d) and becomes $\langle P_{ab} \rangle$=0.60 d (σ=0.05 d) if we only consider 15 RRab's within the r_h convolved with the galaxy ellipticity, while it is $\langle P_{ab} \rangle$=0.60 d (σ=0.05 d) for the 32 RRab's within twice the r_h. In any case, And XXV is classified as an Oosterhoff-

[1] $B - b = 27.696 - 0.113 \times (b - v)$ r.m.s=0.03,
$V - v = 27.542 - 0.060 \times (b - v)$ r.m.s=0.03

Table 2: Identification and properties of the variable stars detected in And XXV. Solid lines separate variable stars located within once and twice the galaxy half-light radius.

Name	α (2000)	δ (2000)	Type	P (days)	Epoch (max) HJD (−2455000)	$\langle B \rangle$ (mag)	$\langle V \rangle$ (mag)	A_B (mag)	A_V (mag)
V1	00:30:10.688	+46:51:21.71	RRab	0.6078	852.561	25.90	25.42	1.10	0.86
V2	00:30:09.937	+46:51:34.93	RRab	0.5459	851.356	25.77	25.38	1.42	0.87
V3	00:30:09.306	+46:51:43.73	RRab	0.6147	852.048	25.80	25.43	1.42	0.86
V4	00:30:12.324	+46:50:58.88	AC	1.355	854.800	24.23	23.79	0.68	0.56
V5	00:30:05.194	+46:50:48.71	RRc	0.3858	851.920	25.82	25.41	0.72	0.36
V6	00:30:11.050	+46:51:58.73	RRab	0.609	854.732	25.58	25.23	0.98	0.76
V7	00:30:05.122	+46:50:27.28	RRab	0.6116	857.708	25.80	25.39	1.00	0.72
V8	00:30:05.122	+46:50:27.28	RRc	0.3457	851.164	25.53	25.17	0.73	0.70
V9	00:30:14.345	+46:50:47.45	RRab	0.5742	856.642	25.57	25.15	1.41	1.10
V10	00:30:04.745	+46:50:06.57	RRab	0.72	854.705	25.71	25.32	0.76	0.49
V11	00:30:14.186	+46:50:17.44	RRab	0.5963	856.705	25.68	25.33	1.06	0.98
V12	00:30:12.939	+46:52:22.79	RRab	0.5466	854.795	25.73	25.39	1.44	1.10
V13	00:30:02.642	+46:50:12.32	RRab	0.7254	852.133	25.80	25.38	1.00	0.78
V14	00:30:02.612	+46:52:23.61	RRab	0.576	854.804	25.72	25.33	1.36	1.06
V15	00:30:14.464	+46:49:28.74	RRab	0.591	856.663	25.63	25.20	1.01	0.79
V16	00:30:17.886	+46:51:58.24	RRab	0.610	851.573	25.95	25.53	0.90	0.56
V17	00:30:18.136	+46:50:05.58	RRab	0.5675	855.784	25.68	25.31	1.36	1.18
V18	00:30:02.457	+46:48:57.10	RRc	0.375	854.810	25.64	25.31	0.74	0.33
V19	00:30:13.024	+46:48:31.33	RRab	0.577	855.587	25.66	25.28	1.22	0.95
V20	00:29:59.216	+46:52:40.02	RRc	0.3085	852.695	25.43	25.16	0.53	0.36
V21	00:30:21.242	+46:51:02.77	RRab	0.562	854.804	25.41	25.07	1.60	1.25
V22	00:29:58.666	+46:53:04.62	RRab	0.655	857.894	25.69	25.31	0.71	0.65
V23	00:30:21.905	+46:51:36.72	RRc	0.3668	858.900	25.49	25.15	0.81	0.61
V24	00:30:18.610	+46:53:37.02	RRab	0.537	854.816	25.66	25.29	1.89	1.28
V25	00:30:15.060	+46:47:56.28	RRab	0.637	856.670	25.73	25.27	0.80	0.51
V26	00:30:23.121	+46:51:10.67	RRc	0.405	856.782	25.61	25.26	0.70	0.47
V27	00:30:21.141	+46:49:12.98	RRab	0.547	857.652	25.60	25.22	1.25	0.97
V28	00:30:17.693	+46:48:10.12	RRab	0.565	856.747	25.62	25.25	1.42	1.12
V29	00:29:55.136	+46:49:28.51	RRab	0.632	856.860	25.73	25.26	0.781	0.56
V30	00:30:03.691	+46:47:25.31	RRc	0.368	856.767	25.55	25.20	0.452	0.41
V31	00:30:13.107	+46:47:15.13	RRab	0.669	856.780	25.50	24.88	0.845	0.51
V32	00:30:11.748	+46:55:04.50	RRc	0.378	856.677	25.60	25.34	0.66	0.59
V33	00:29:58.771	+46:47:48.94	RRab	0.577	856.850	25.61	25.24	0.87	0.72
V34	00:30:26.025	+46:51:13.58	RRab	0.5575	858.894	25.65	25.30	1.16	0.81
V35	00:30:19.772	+46:47:45.21	RRab	0.579	854.780	25.64	25.17	1.50	1.17
V36	00:30:26.764	+46:50:36.83	RRab	0.5678	858.615	25.47	25.14	1.71	1.32
V37	00:30:02.239	+46:46:45.76	RRab	0.6992	857.747	25.64	25.23	0.80	0.62
V38	00:30:18.484	+46:47:02.00	RRab	0.67	856.802	25.63	25.30	0.72	0.47
V39	00:30:22.544	+46:54:27.27	RRab	0.5766	858.601	25.54	25.22	1.21	1.00
V40	00:30:18.502	+46:46:50.06	RRab	0.621	858.638	25.66	25.27	1.37	0.82
V41	00:29:55.859	+46:47:19.20	RRab	0.618	856.664	25.66	25.29	0.82	0.67
V43	00:29:48.512	+46:51:50.74	RRc	0.37	855.660	25.59	25.17	0.64	0.34
V44	00:29:48.589	+46:49:46.67	RRab	0.615	858.598	25.59	25.25	0.92	0.69
V45	00:30:04.316	+46:44:45.19	RRab	0.5867	855.842	25.59	25.33	1.13	0.93
V46	00:29:42.803	+46:51:51.83	AC/CC?	1.213	852.697	23.82	23.38	0.62	0.40
V47	00:30:08.635	+46:44:29.81	RRab	0.6322	854.715	25.65	25.36	1.02	0.81
V48	00:29:57.962	+46:44:56.31	RRab	0.6325	857.792	25.74	25.36	0.81	0.70
V49	00:30:25.549	+46:56:26.38	RRab	0.592	855.790	25.65	25.33	1.05	0.92
V50	00:29:41.661	+46:50:24.07	RRab	0.579	856.863	25.65	25.45	0.81	0.67
V51	00:30:17.641	+46:57:49.18	RRab	0.6371	855.593	25.43	25.08	1.13	0.93
V52	00:30:09.862	+46:43:59.74	RRab	0.6243	856.652	25.58	25.20	0.97	0.71
V53	00:30:20.789	+46:44:32.70	RRc?	0.3934	854.826	25.54	25.26	0.56	0.42
V54	00:30:24.470	+46:57:13.95	RRab	0.635	855.580	25.66	25.20	0.80	0.65
V55	00:30:37.347	+46:52:57.46	RRab	0.681	851.572	25.61	25.231	0.80	0.66
V56	00:29:50.346	+46:44:58.80	RRc	0.299	858.907	25.66	25.39	0.67	0.53
V57	00:30:16.060	+46:42:25.70	RRab	0.57	856.764	25.77	25.38	0.97	0.72
V58	00:29:32.588	+46:49:37.73	AC	0.531	855.810	24.53	24.24	0.90	0.76
V59	00:29:56.648	+46:42:10.13	RRab	0.642	856.847	25.45	25.22	1.201	1.087
V60*	00:30:13.652	+46:41:30.72	uncl	0.848	854.595	21.48	19.96	0.239	0.197
V61*	00:30:06.316	+46:41:26.44	ECL	0.25677	856.760	24.24	23.22	1.39	0.886
V62	00:30:14.030	+46:41:22.26	RRab	0.5337	856.732	25.67	25.22	1.58	1.233
V63*	00:29:49.898	+46:49:07.68	RRab	0.5486	855.629	25.55	25.16	1.483	1.157

*Field variable stars

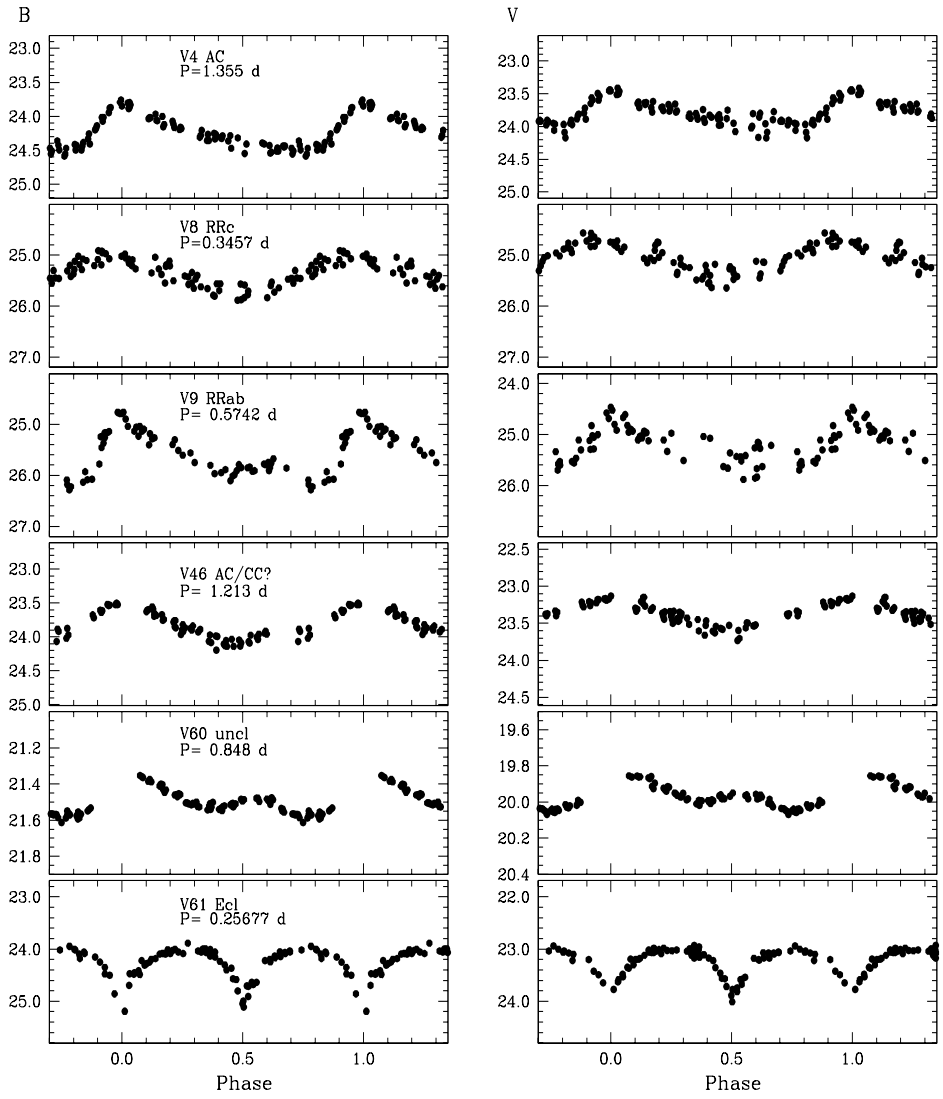

Fig. 1.— Examples of B-band (left panels) and V-band (right panels) light curves for different types of variable stars identified in And XXV. Typical internal errors of the single-epoch data range from 0.01 at $B \sim 21.30$ mag (corresponding to the maximum light of the unclassified variable V60) to 0.30 mag at $B \sim 26.20$ mag (corresponding to the minimum light of the fundamental mode RR Lyrae V9), and similarly, from 0.01 mag at $V \sim 19.90$ mag to 0.30 mag at $V \sim 26.00$ mag.

Intermediate (Oo Int) system (Oosterhoff 1939; Catelan 2009).

The fraction of RRc stars in And XXV over the whole number of RR Lyrae stars is $f_c = N_c/N_{ab+c} = 0.21 \pm 0.07$, that is intermediate between what expected for Oosterhoff II (Oo II; $f_c \sim 0.44$) and Oosterhoff I (Oo I; $f_c \sim 0.17$) systems (Catelan 2009), again confirming the classification of And XXV as Oo Int.

The period-amplitude diagram (also known as Bailey diagram, Bailey 1902) of the RR Lyrae stars in And XXV is shown in the left panel of Figure 3 together with the loci defined by RR Lyrae stars in the Oo I Galactic globular cluster M3 (lower line) and the Oo II globular cluster ω Cen (upper line), according to Clement & Rowe (2000). We separated the RR Lyrae stars in three groups depending on the position inside once and twice the area delimited by the r_h convolved with the galaxy ellipticity, and in the whole LBC field of view (FOV). Almost all RR Lyrae stars fall on the Oo I locus or between the two lines but keeping closer to the Oo I position. Only three RR Lyrae stars are near the Oo II locus. In the right panel of Figure 3 the period-amplitude diagram of And XXV's RR Lyrae stars is compared to the distribution of RR Lyrae in And XIX, And XXI and in three halo fields at 4, 6 kpc (Sarajedini et al. 2009) and 35 kpc (Brown et al. 2004) from the center of M31, respectively. The RR Lyrae stars in the M31 halo conform more to the Oo I type, while the dwarf Spheroidal galaxy (dSph) satellites are more Oo Int with a slight trend towards Oo I type, which decreases with increasing the distance from the M31 center.

The RR Lyrae stars trace the old populations of a galaxy and from their positions is thus possible to draw a first picture of the geometry of And XXV. The spatial distribution of the RR Lyrae stars in And XXV is shown in Figure 4 (filled red circles), and reveals the elongated structure of this galaxy. Adopting the structural parameters derived by Richardson et al. (2011), many RR Lyrae stars appear to be placed beyond the galaxy half-light radius, traced by the inner black ellipse, and create a protrusion of stars that extends beyond twice the r_h. In particular, more than half of the RR Lyrae stars (37 out of 57) are located southward with respect to the galaxy center and suggest a stretched distribution

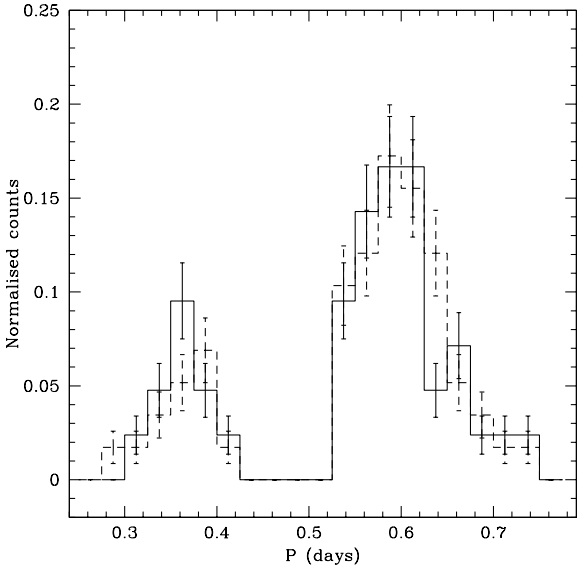

Fig. 2.— The dashed histogram represents the distribution of the periods of all the RR Lyrae stars identified in And XXV. The continuous line histogram is for RR Lyrae enclosed in twice the galaxy r_h. The bin size is 0.025 days.

of And XXV's stars. Most of them are aligned along the direction toward M31.

3.2. ANOMALOUS CEPHEIDS

In And XXV we identified three variable stars, namely, V4, V46 and V58, that fall inside the instability strip (see Marconi et al. 2004), but have luminosities exceeding the average magnitude of the RR Lyrae stars by about 1 mag. Following the procedure discussed in Papers I and II, by the cross study with isochrones in the CMD, the period-Wesenheit (PW) relations for ACs and classical Cepheids (CCs) and the analysis of the light curves we classify these three stars as ACs. However the classification for the star V46 is more uncertain and this star can be also seen as a short period CC.

To obtain the Wesenheit index of these 3 variables we subtracted the color term multiplied by 3.1 (adopting the Cardelli et al. 1989, law for extinction) to the absolute magnitudes derived by their intensity-averaged apparent visual magnitudes, $\langle V \rangle$, adopting the distance modulus of (m-

M)$_0$=24.63 ± 0.17 mag as derived from the RR Lyrae stars (see Section 4). In the left panel of Figure 5 are displayed the *PW* relations for ACs in the Large Magellanic Cloud (LMC, solid lines) derived by Ripepi et al. (2014)[2]. V4, V46 and V58 fall within 1σ of the Ripepi et al. (2014) relations for fundamental mode and first-overtone pulsators. In the right panel of Figure 5 we compare the three variables with the *PW* relations of the LMC CCs by Jacyszyn-Dobrzeniecka et al. (2016). Clearly, V4 does not fit the CC *PW* relations, while both V46 and V58 are within 1 σ of the fundamental mode CC *PW*. However, looking at the shape of the light curve V58 shows the typical trend variation of an AC (see Paper I and II for examples). Therefore, we finally classify V58 as AC, while for V46 we give an intermediate classification between AC and CC. Since both V46 and V58 are outside twice the area defined by the galaxy r$_h$, they could either belong to a background/foreground feature of the M31 field, or could be recently formed stars due to a peripheral episode of star formation in And XXV triggered by tidal interaction. In any case, given the uncertain membership of V46 and V58, we have computed the specific frequency of ACs in And XXV under the assumption that V4 is the only AC belonging to the galaxy. This is shown in Figure 6 together with the AC specific frequency in a number of MW and M31 dwarf satellites. And XXV does not follow the relation traced by the other galaxies. Moreover, to make a more consistent comparison between the ACs discovered in this paper, in Papers I and II, and those presented in other studies (Pritzl et al. 2005, and reference therein), we have revised the AC specific frequency in dwarf galaxies analyzed in those previous studies, considering as bona fide ACs only those falling within 1 σ of the PW relations for ACs. This tool has confirmed the AC number in the following satellites: Leo I, Leo II, Draco, Ursa Minor, Carina, Sculptor, and Fornax but has reduced it in And I and And II (from 1 to 0), And III (from 5 to 2), And VI (from 6 to 4) and Sextans (from 4 to 2). The red solid lines plotted in both panels of Figure 6 are the least-square fits obtained adopting the revised specific frequencies computed as discussed above. They are described by the following equations:

$$\log S = 0.23(\pm 0.57) \times Mv + 2.22(\pm 0.57) \quad (1)$$

$$\log S = -1.39(\pm 0.44) \times [Fe/H] - 2.62(\pm 0.83) \quad (2)$$

Black lines mark instead the least-square fits originally obtained in Pritzl et al. (2005).

Grey dashed arrows indicate the position the revised galaxies would occupy in these plots if we used their literature AC specific frequencies. In the right panel new and previous fits are in perfect agreement, while in the left panel the slope of the new fit is less steep indicating that for fainter galaxies a smaller number of ACs is expected.

3.3. OTHER VARIABLES

In the field of And XXV we discovered two variable stars, namely, V60 and V61, that in the CMD (Figure 7) are outside the instability strip for Cepheids and RR Lyrae stars (Marconi et al. 2004). V61 was classified by the light curve analysis as an ECL, while we were unable to give a clear classification for V60. The position in the CMD (see Figure 7) and the projected spatial distribution (Figure 4) suggest them to belong more likely to the M31 field or to Milky Way (MW). V60 in particular, with a $B - V \sim 1.5$ mag and a V 20 mag is a field star, beyond any doubts.

4. DISTANCE

The V average magnitude of the whole sample of RR Lyrae stars in And XXV is $\langle V(RR) \rangle = 25.26 \pm 0.10$ mag (average on 57 stars). If we exclude V31 that is 0.39 mag brighter than the RR Lyrae average magnitude and can be either a blended star or an evolved RR Lyrae we obtain $\langle V(RR) \rangle = 25.27 \pm 0.09$ mag. Considering instead the subsample of RR Lyrae inside an area delimited by And XXV r$_h$ the average V magnitude is $\langle V(RR) \rangle = 25.33 \pm 0.09$ mag (average on 18 stars). As for Paper I and II, to correct for interstellar extinction we derived the reddening from the galaxy RR Lyrae stars adopting the method described by Piersimoni et al. (2002). For the sample of RR Lyrae within the r$_h$, the reddening is $E(B-V) = 0.08 \pm 0.04$ mag, for the whole sample $E(B-V) = 0.05 \pm 0.04$ mag. These values are slightly smaller than derived by Schlegel et al. (1998, $E(B-V) = 0.10 \pm 0.06$ mag), but still

[2]Ripepi et al. (2014)'s relations were derived for the V and I bands, and we have converted them to B and V using equation 12 of Marconi et al. (2004).

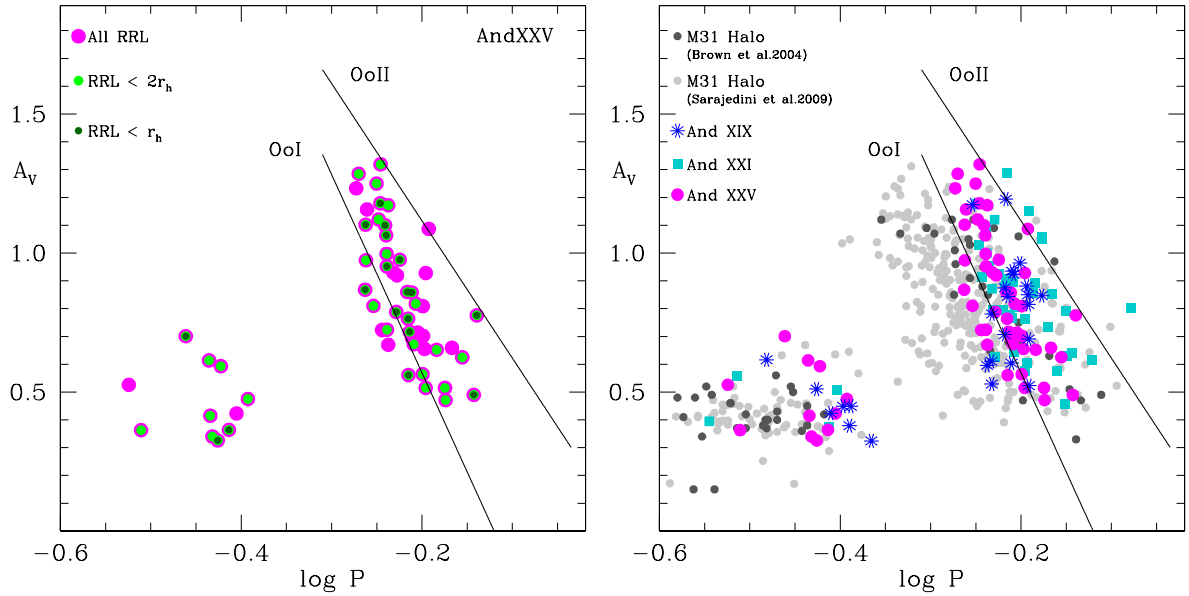

Fig. 3.— *Left*:Period-amplitude diagram of the RR Lyrae stars in And XXV. The solid lines are the ridge lines of the Oo I and Oo II RR Lyrae stars (Clement & Rowe 2000). Dark and light green circles are the RR Lyrae stars inside once and twice the r_h of the galaxy, respectively. Purple circles are all the RR Lyrae stars. *Right*: Same as in the left panel combined with the RR Lyrae stars in And XIX (blue asterisks), And XXI (cyan squares) and in three HST fields in the M31's halo from Sarajedini et al. (2009) (grey symbols) and Brown et al. (2004) (dark-grey symbols), respectively.

consistent within 1 σ. To compute the distance to And XXV we adopt the average V magnitude and reddening obtained from the RR Lyrae inside the r_h, $M_V = 0.54 \pm 0.09$ mag for the absolute visual magnitude of RR Lyrae stars with metallicity of [Fe/H] $= -1.5$ dex (Clementini et al. 2003) and $\frac{\Delta M_V}{\Delta [Fe/H]} = -0.214 \pm 0.047$ mag/dex (Clementini et al. 2003; Gratton et al. 2004) for the slope of the RR Lyrae luminosity-metallicity relation. For the metallicity of And XXV we adopt the value [Fe/H]$=-1.9 \pm 0.1$ dex as derived spectroscopically by Collins et al. (2013). The distance modulus of And XXV derived from the RR Lyrae stars is thus $(m\text{-}M)_0$=24.63±0.17 mag. This estimate is in very good agreement with the result of Richardson et al. (2011), $(m\text{-}M)_0$=24.55 ± 0.12 mag, who used the luminosity of the HB to infer the galaxy distance, but it is more than 1σ longer than obtained by Conn et al. (2012), $(m\text{-}M)_0 = 24.33^{+0.07}_{-0.21}$ mag, who used the luminosity of the RGB tip. We suspect that the distance derived in Conn et al. (2012) might be hampered by the uncertain location of the RGB tip which is scarcely populated in And XXV.

5. CMD AND STELLAR POPULATIONS

The CMD of And XXV is shown in Figure 7, where in the left panel are plotted only sources located within the area delimited by the galaxy half-light radius and the ellipticity given by Richardson et al. (2011), in the central panel are displayed sources enclosed between once and twice the r_h, whereas the right panel shows the CMD of sources in the whole LBC FOV. We minimized the presence of background galaxies and peculiar sources by selecting only sources with DAOPHOT quality image parameters $-0.35 \leq$ Sharpness ≤ 0.35 and $\chi < 1.5$. Red filled circles are the RR Lyrae stars, green filled triangles are the ACs (the open green triangle is the uncertain AC/CC), the blue pentagon is the unclassified variable, while the ECL is marked by a black asterisk. The main features of the CMD are the RGB and the HB traced by the RR Lyrae stars.

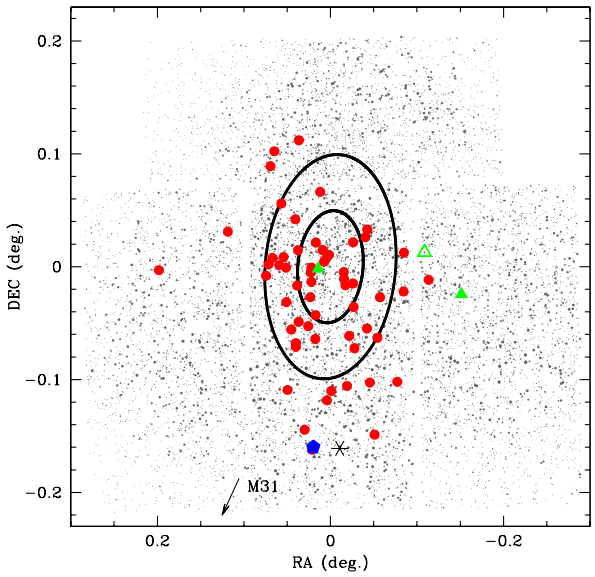

Fig. 4.— Spatial distribution of the variable stars discovered in the whole LBT FOV. The black ellipses represent the area enclosed respectively by once and twice the r_h of And XXV defined by Richardson et al. (2011). Red filled circles mark the RR Lyrae stars, green filled triangles the ACs, open green triangle is the uncertain AC/CC, the blue pentagon is the unclassified variable and the black asterisk is the ECL. The arrow points to the direction of M31.

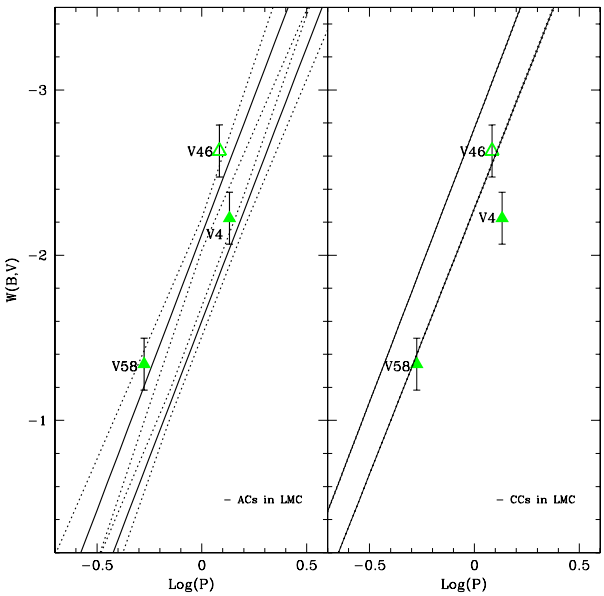

Fig. 5.— Position of V4, V46 and V58 with respect to the PW relations for ACs (left panel; Ripepi et al. 2014) and CCs in the LMC (right panel; Jacyszyn-Dobrzeniecka et al. 2016). The 95% confidence contours are shown as dotted lines. For the CCs the errors of the fits are very small and the condifence contours are very close to the fits.

The majority of stars filling up the redder part of the CMD at $B - V \sim 1.5 - 1.7$ mag and going beyond $V = 22$ mag are foreground field objects. V60, the unclassified variable located in this region of the CMD is most probably a field variable star belonging to the MW field.

The narrow RGB and the poorly populated red HB suggest that And XXV hosts a dominant single old stellar population. In Figure 8 the CMD features and the position of the variable stars are compared with Padua isochrones obtained using the CMD 2.5 web interface ($http://stev.oapd.inaf.it/cgi-bin/cmd$) based on models from Bressan et al. (2012). Isochrones for ages from 9 to 13 Gyr and metallicity Z=0.0003-0.0004 fit well the RGB and the position of the RR Lyrae stars. The red HB is also well fitted by the isochrones in these age and metallicity ranges.

The only AC discovered within twice the r_h of And XXV can either be the result of coalescence in a binary system as old as the RR Lyrae stars, in which mass transfer acted in the last Gyr, or an intermediate young (1-2 Gyr old) star with metallicity in the range Z=0.0001-0.0006 (as widely discussed in Paper I and Paper II). The paucity of ACs in And XXV gives indication that there is lack of a young/intermediate age stellar population in this galaxy, when compared to And XIX and And XXI. We selected stars in the CMD of sources in the whole LBC FOV that have color and magnitude in the range of ACs ($0.2 \leq B - V \leq 0.6, 23.0 \leq V \leq 24.5$) and we did not find any clear distribution/concentration of stars associated with this selection. The star formation in And XXV most probably was quenched by some external event as, for instance, tidal stripping by large nearby galaxies like the NGC147/NG185 pair (see

next Section) or from M31 itself. In this scenario, the presence of at least one CC and one AC off-centered with respect to And XXV could indicate that a mild recent activity has been triggered from the outside.

5.1. PROJECTED SPATIAL DISTRIBUTIONS

RGB stars were selected from the CMD in the right panel of Figure 7, showing stars contained in the whole LBT FOV. The selection performed is marked with a magenta region in Figure 7. The RGB isodensity contours are shown in the left panel of Figure 9 and reveal very interesting features of And XXV structure.

Moving outwards from the galaxy center, the outermost contours appear to be elongated toward the position of NGC147 and NGC185, the major axis direction of the isodensity contours changes, and finally points towards the direction of these two galaxies. Since isodensity twisting is mainly due to tidal effects (di Tullio et al. 1979; Johnston et al. 2002), we suggest that And XXV is likely experiencing tidal stirring from the relatively nearby couple NGC147/NGC185 on one side and from M31 in the orthogonal direction. Perhaps, And XXV is infalling the M31 halo for the first time and feeling both the tidal force of the NGC147/NGC185 couple and of the massive host galaxy M31. Projected distances to NGC147/NGC185 and M31 are ∼95 kpc and ∼ 143 kpc, respectively, (adopting distances reported in Conn et al. 2012 for these systems). The right panel of Figure 9 shows the spatial distribution of the HB stars. This part of the CMD is heavily contaminated by background unresolved galaxies. Nevertheless it is still possible to see some of features traced by the RGB isodensities. A protrusion of HB stars extending in the direction of the M31 center highlights the tidal interaction between And XXV and M31.

6. GEP I: AND XXV's CENTER OR A NEW GLOBULAR CLUSTER ORBITING AND XXV OR M31?

Visual inspection of the deep image obtained by stacking all the B-band LBC frames (for a total of 9.4 hours integration time) has revealed a spherical assembly of stars near And XXV's photometric center, that we named Gep I[3]. This serendipity discovered concentration of stars is centred around coordinates R.A.=00:30:10.579 dec.=+46:51:05.58 and is of ∼ 12 arcsec in diameter. A snapshot of Gep I from our deep LBT B-band image is shown in Figure 10. In the discovery paper Richardson et al. (2011) note that And XXV falls close to the 2 arcmin gaps among CCDs in their observations (see Fig. 2 of Richardson et al. 2011) significantly hampering the determination of And XXVs centroid, for which they estimate a quite large ∼12 arcsec uncertainty. The difference between Gep I and And XXV center coordinates is ∼11 arcsec, hence, Gep I is within the error box of Richardson et al. (2011) center coordinates of the galaxy.
The stellar concentration could either be And XXV actual center or a new star cluster belonging to And XXV or M31. Indeed, there is no known Globular Cluster (GC) in the Revised Bologna Catalogue of the M31 GCs (Galleti et al. 2004), nor any other known extended source within ∼20 arcsec of Gep I center coordinates. Integrated photometry of Gep I was performed using GAIA (Graphical Astronomy and Image Analysis Tool) starting from the center of the cluster and with circular apertures ranging from 1 to 20 arcsec radius. With this method we estimated the half light radius of Gep I to be $r_h \sim 6$ arcsec and its integrated magnitudes, computed within twice the r_h, are B ∼20.6 mag and V ∼20.0 mag, respectively. Assuming the distance modulus and reddening of And XXV, we obtain absolute magnitudes of $M_B \sim -4.2$ mag and $M_V \sim -4.9$ mag, respectively. The r_h of Gep I at the distance of And XXV corresponds to ∼25 pc in linear extension. Radius and absolute V magnitude place Gep I in the region of the $M_V - r_h$ plane that seems forbidden to ordinary GCs. Only the M31 Extended Clusters (ECs, Huxor et al. 2011) and the least luminous among the MW Palomar GCs are found to lie in this region (see Figure 10 of Huxor et al. 2011) along with the nuclei of dwarf elliptical galaxies. This leaves open the possibility that Gep I could indeed be the center of And XXV.

The stars that our photometry could resolve in this cluster are just a few and their position in

[3]In the memory of a young colleague of us, Geppina Coppola, prematurely passed away.

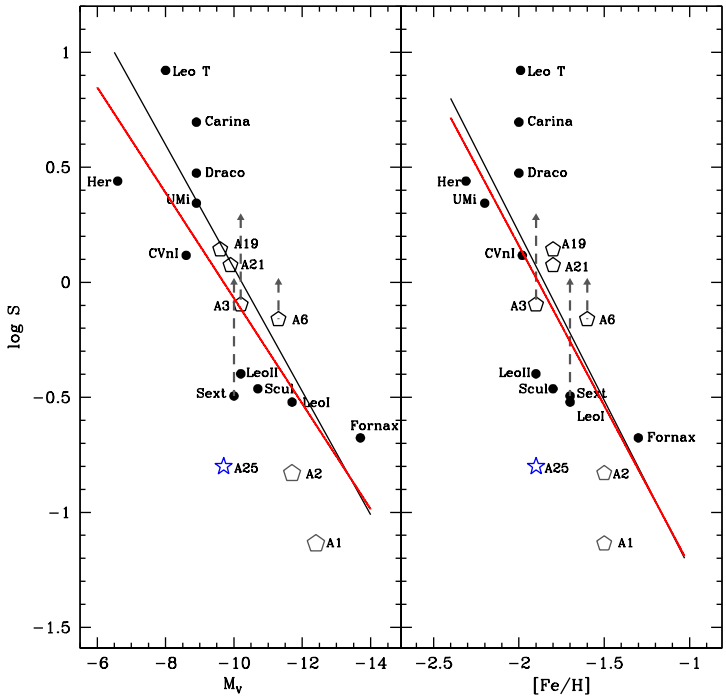

Fig. 6.— *Left*: Specific frequency of ACs in dwarf satellites of the MW (filled circles) and M31 (open pentagons) versus absolute visual magnitude. And XXV is represented by the blue star. Black lines are the least-squares fits of ACs by Pritzl et al. (2005) while the red solid lines mark the least-squares fits we have been obtaining using only ACs confirmed by the comparison with the PW relations for ACs (see text for details). *Right*: Same as in the left panel, but versus metallicity of the parent galaxy.

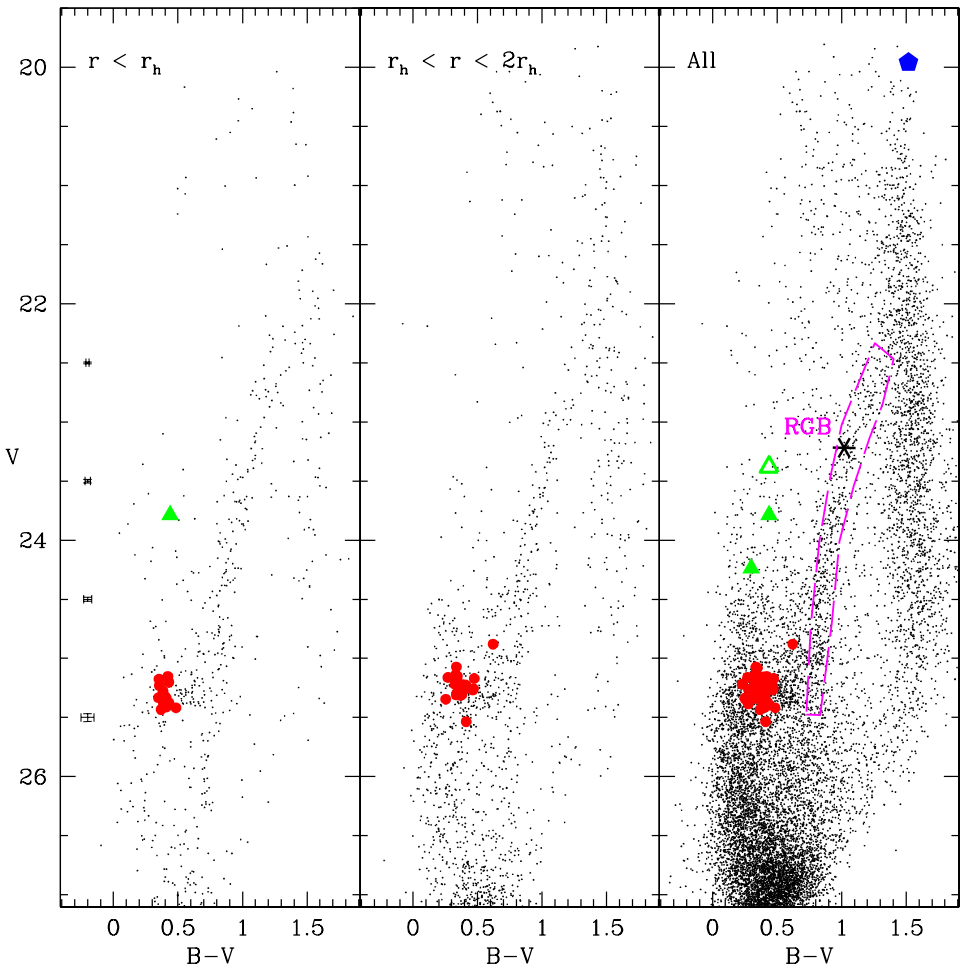

Fig. 7.— *Left*: CMD of sources in our photometric catalog with $-0.35 \leq$ Sharpness ≤ 0.35 and with $\chi < 1.5$ and located within the area delimited by the galaxy half-light radius and the ellipticity by Richardson et al. (2011). Red circles mark the RR Lyrae stars while green triangles are the ACs. *Center*: Same as in the left panel, but within the area between once and twice the galaxy r_h. *Right*: As in the left panel, but considering sources in the whole LBC FOV. The black asterisk is the ECL, the blue pentagon is the unclassified variable, while the open green triangle is the uncertain AC/CC.

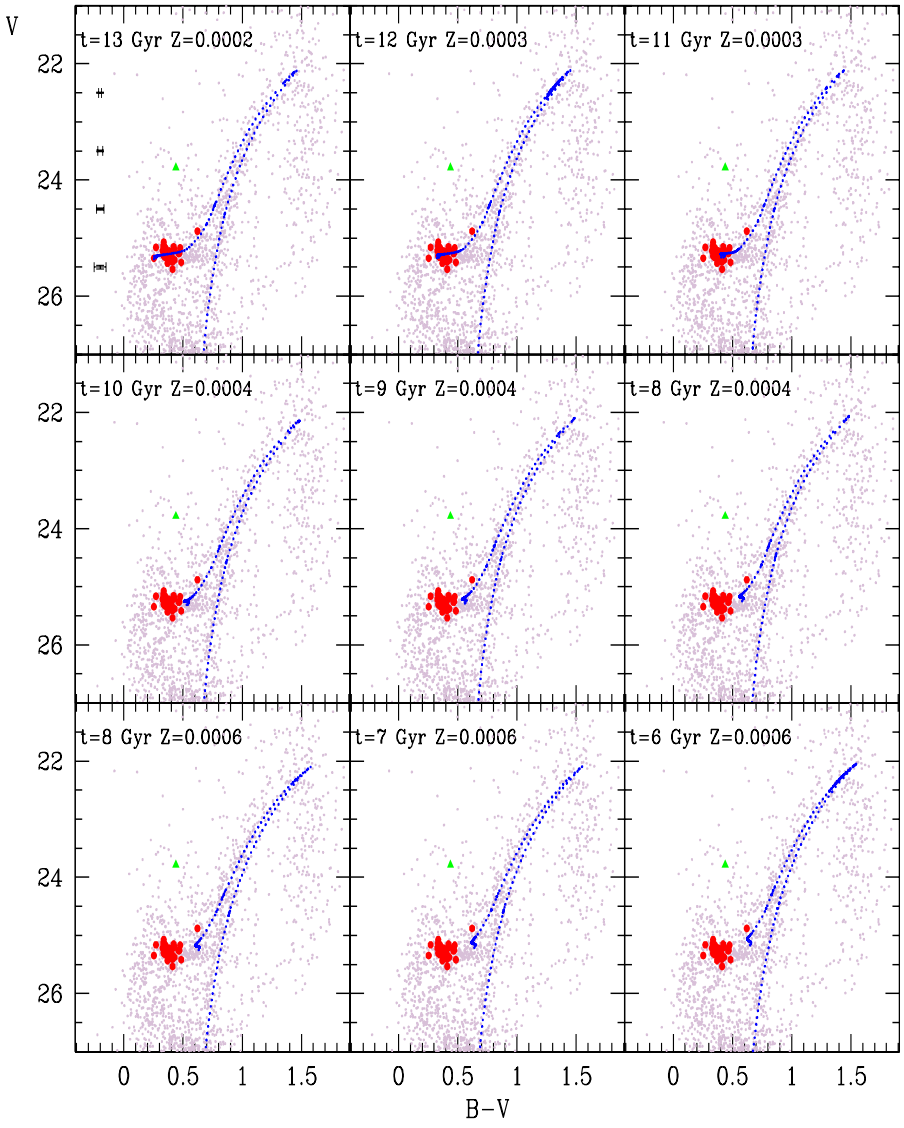

Fig. 8.— CMD of sources contained within twice the r_h of And XXV, overlaid by Padua stellar isochrones (Bressan et al. 2012) with different age (from t=13 Gyr to 6 Gyr) and metallicity (Z=0.0003, Z=0.0004 and Z=0.0006; from top to bottom). Red filled circles are RR Lyrae stars, the green filled triangle is the AC (V4).

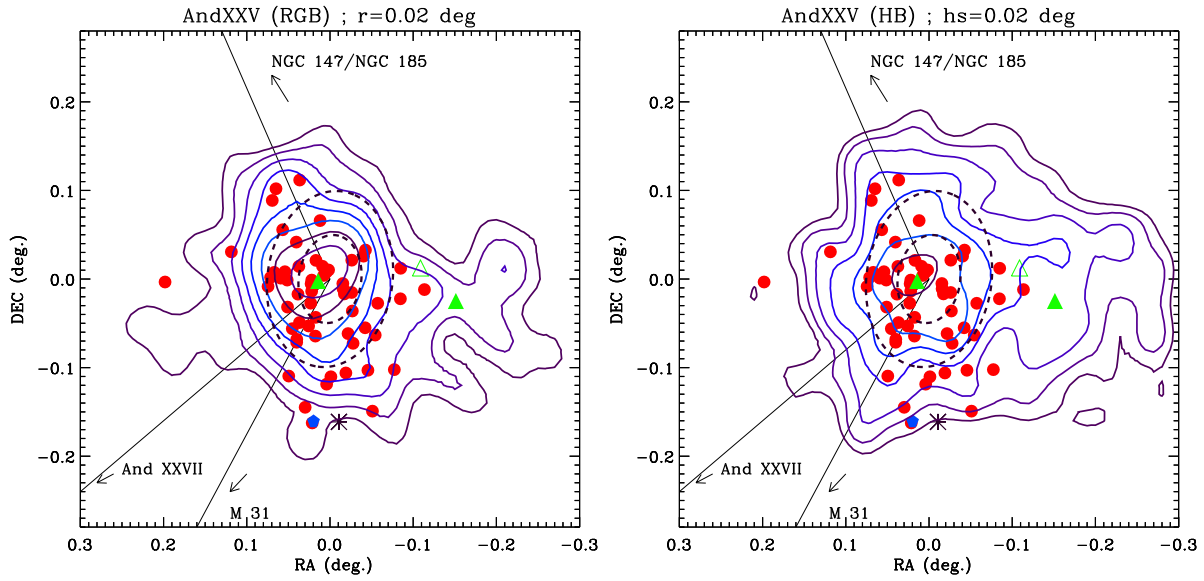

Fig. 9.— *Left*: Isodensity contours of RGB stars in And XXV. RA and DEC are the differential coordinates computed from the center of the galaxy given by Richardson et al. (2011). The black dashed ellipses mark the areas within once and twice the r_h. The variable stars are shown with different colors and symbols (red circles for RR Lyrae stars, green filled triangles for ACs (open green triangle for the uncertain AC/CC), black asterisks for the ECL, blue pentagon for the unclassified variable). *Right*: Same as in the left panel but for And XXV HB stars.

the CMD is shown in the left panel of Figure 11. This CMD was done taking all the objects in a circular area of 12 arcsec in radius from the center of the stellar association (field F1). These stars are mostly red giants with only one or two HB stars. Their location in the CMD is compatible with an old population placed at a Heliocentric distance of ∼750-800 kpc. Center and right panels of Figure 11 show, for a comparison, the CMDs of sources in two circular regions F2 (central panel) and F3 (right panel) of a radius equal twice the estimated r_h of Gep I, but centered ∼1 arcmin to the North-West and ∼ 1 arcmin to South-East with respect of the F1 centre, respectively. The positions of F2 and F3 in the LBC FOV are marked with red circles in Figure 10. The CMDs of fields F2 and F3 show no clear evidence of a single old stellar population similar to the one observed in field F1, thus confirming that in F1 there is a real concentration of old stars. Cleary, this ground-based CMD of Gep I is severely incomplete.

To unveil the nature of Gep I we have proposed follow up HST observations in order to resolve and characterize its stellar populations and precisely measure its distance. If the concentration of stars is proven to be a GC belonging to And XXV the galaxy would be one of the few dSphs in the Local Group known to host GCs, after Fornax and Sagittarius.

Moreover, the position of this putative GC very close to the center of And XXV (according to Richardson et al. 2011 coordinates), would resemble the case of M54 which is in the core of its parent galaxy, the Sagittarius dSph according to Monaco et al. (2005). Very recently a stellar cluster has been detected near the center of the Eridanus II dwarf galaxy by Crnojević et al. (2016). The authors claim that Eridanus II is the faintest galaxy to host a stellar cluster. In the same vein, And XXV could be the faintest galaxy of the M31 complex to host a stellar cluster.

Zaritsky et al. (2016) have suggested that most GCs may be hosted by undetected faint galaxies. Our discovery in And XXV along with Crnojević et al. (2016)'s discovery of the cluster in Eridanus II may lend support to Zaritsky et al. (2016)'s claim and provide hints on the connection

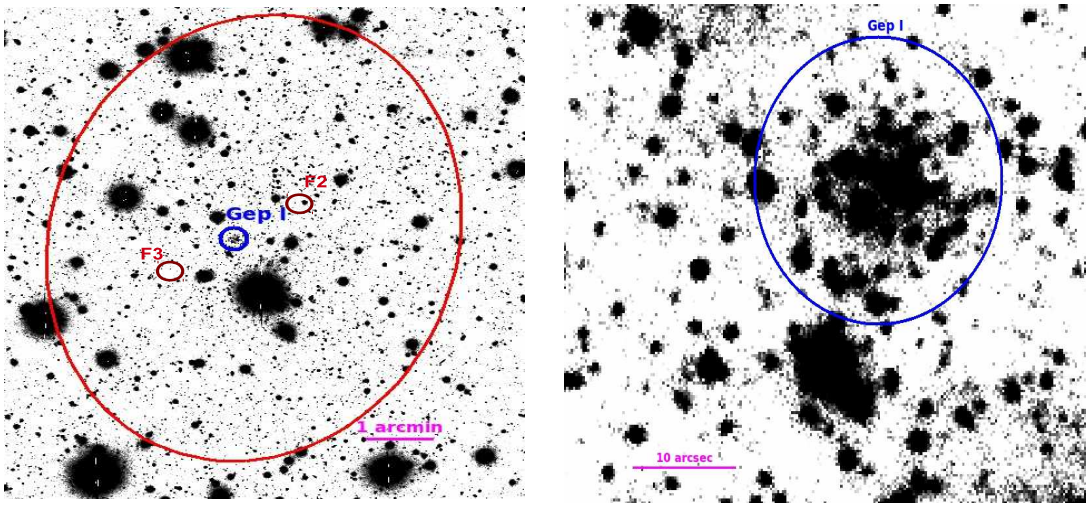

Fig. 10.— *Left*: Part of the deep image obtained by stacking all B-band frames. The position of Gep I is highlighted with a blue circle. The positions of the comparison fields F2 and F3 are marked with red circles. The concentration of stars is near the center of And XXV, the red ellipse shows the area delimited by once the r_h. North is up and East to the left. *Right*: a closed in view of Gep I.

between GCs and dwarf galaxies.

7. SUMMARY AND CONCLUSIONS

Based on B, V time series photometry obtained with LBCs at LBT we have discovered 63 variable stars in the field of And XXV dSph, of which 58 are RR Lyrae stars, 3 are ACs, 1 is an ECL and 1 is an unclassified variable. The average period of the RRab stars classifies this galaxy as an Oosterhoff intermediate object. The comparison of the galaxy CMD with isochrones and the population of variable stars are compatible with a single old (9 -13 Gyr) and metal poor ([Fe/H]~ -1.8 dex) stellar generation being the predominant component of And XXV. In the field of And XXV we have detected a spherical concentration of stars near the galaxy center that could either be a candidate globular cluster or the center of the galaxy. And XXV is the first of the M31 satellites we have investigated so far to lay on the Great plane of Andromeda (GPoA) defined by Ibata et al. (2013). The stellar populations detected in And XXV differ somehow from the stellar populations we have identified in And XIX and And XXI, which both lay off the GPoA. In particular, in And XXV there is lack of an intermediate/young stellar population, compared to And XIX and And XXI, and a very small number of ACs. Besides And XXV, only four other M31 satellites on the GpoA have been investigated so far to detect variable stars and have a metallicty [Fe/H]≤ -1.5 dex (which is the condition to generate ACs, see e.g. Marconi et al. 2004), namely: And I, And III (Pritzl et al. 2005), And XI and And XIII (Yang & Sarajedini 2012). Pritzl et al. (2005) found no ACs in And I and two ACs in And III (following our re-analysis in Section 3.2), while in And XI and And XIII no ACs were detected. Although at present the statistic is still rather meager (5 out of 15 satellites laying on the plane) it seems that galaxies on the GPoA have no or very few ACs, hence, that they host no or very few intermediate-age stars[4].

We have compared the pulsation properties of the RR Lyrae population in the M31 dSph satellites on and off the GPoA. The M31 dSphs that have been studied for variability are listed in the Table 3 along with their membership to the GPoA and the characteristics of their RR Lyrae populations. The average period of RRab stars for galaxies on and off the plane is $\langle P_{ab}\rangle$=0.62 $\pm$ 0.07 d and

[4]We note that And XVI, a galaxy located at a projected distance of d_{M31}=323 kpc from the M31 center, but offset by only 8 kpc from the GPoA (Pawlowski et al. 2013), also does not seem to contain ACs (Monelli et al. 2016).

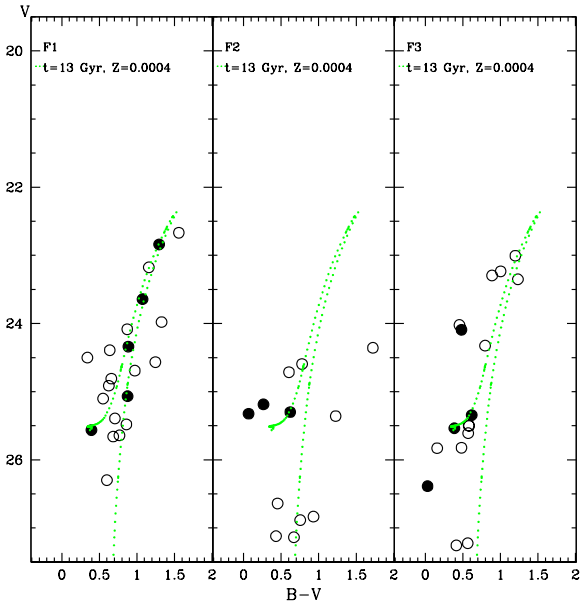

Fig. 11.— *Left*: CMD of sources in a circular area within a radius of 12 arcsec from the center of Gep I (field F1). Filled circles are sources in our LBC photometric catalog selected using the DAOPHOT χ and Sharpness parameters (-0.35 $\leq$ Sharpness $\leq$ 0.35 and $\chi < 1.5$). The green dashed line is an isochrone with t=13 Gyr and Z=0.0004 from Bressan et al. (2012). *Center*: same as in the left panel but for sources in F2. *Right*: same as in the left panel for sources in F3.

$\langle P_{ab} \rangle$=0.60 $\pm$ 0.06 d, respectively. The fraction of RRc to the total number of RR Lyrae stars is f_c=0.31 and f_c=0.23 for on and off plane satellites. Both populations are thus compatible with an Oo-Int classification, but with a slight tendency towards Oo-II type for the on plane satellites. In Figure 12 we plot the cumulative period distribution of the RR Lyrae stars in the two samples. A two-sample Kolmogorov-Smirnov (K-S) test was performed to check if there are significant differences between the two populations. The p-value of the K-S test is p= 0.36 and at this level of the investigation we cannot reject the hypothesis that the two RR Lyrae populations have very similar pulsation properties. For the ACs distribution instead there is a clear difference considering that the total number of ACs for on plane galaxies is 3 while this number for the off plane galaxies is 21

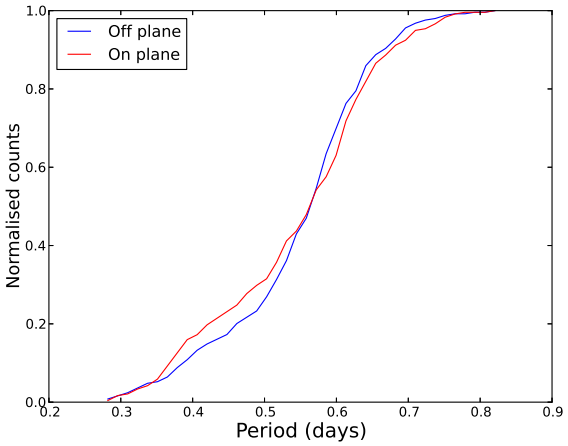

Fig. 12.— Cumulative period distribution of the RR Lyrae stars in M31 satellite galaxies on and off the GPoA.

(see Table 3 column 6). From the variable stars we can thus perhaps draw a first picture of the M31 satellite complex, in which all satellites had a common ancient star formation episode about 10-12 Gyr ago that led to the formation of the RR Lyrae stars. After that, the evolution history of on and off plane satellites started to differentiate and only the latter were able to retain enough gas to produce an intermediate-age stellar population that also gave rise to significant numbers of ACs.

We warmly thank P. Montegriffo for the development and maintenance of the GRATIS software. Financial support for this research was provided by PRIN INAF 2010 (PI: G. Clementini) and by Premiale LBT 2013. The LBT is an international collaboration among institutions in the United States, Italy, and Germany. LBT Corporation partners are The University of Arizona on behalf of the Arizona university system; Istituto Nazionale di Astrofisica, Italy; LBT Beteiligungsgesellschaft, Germany, representing the Max-Planck Society, the Astrophysical Institute Potsdam, and Heidelberg University; The Ohio State University; and The Research Corporation, on behalf of The University of Notre Dame, University of Minnesota, and University of Virginia. We acknowledge the support from the LBT-Italian Coordination Facility for the execution of observations, data distribution, and

Table 3: Properties of the variable stars in the Andromeda satellite galaxies

Name	N (RRab+RRc)	$\langle P_{ab} \rangle$	f_c	N (AC)	N (AC) confirmed*	member	Reference
And I	72+26	0.57	0.26	1?	0	yes	(1)
And II	64+8	0.57	0.11	1	0	no	(2)
And III	39+12	0.66	0.23	5?	2	yes	(1)
And VI	91+20	0.59	0.18	6	4	no	(3)
And XI	10+5	0.62	0.33	0	0	yes	(4)
And XIII	12+5	0.66	0.30	0	0	yes	(5)
And XVI	3+6	0.64	0.33	0	0	no[1]	(5,6)
And XIX	23+8	0.62	0.26	8	8	no	(7)
And XXI	37+4	0.63	0.10	9	9	no	(8)
And XXV	46+12	0.60	0.21	2	1	yes	(9)

* see Section 3.2

[1] offset by 8 Kpc from the GPoA

(1) Pritzl et al. (2005); (2) Pritzl et al. (2004); (3) Pritzl et al. (2002); (4) Yang & Sarajedini (2012);

(5) Mercurio et al. (2016, in preparation);(6) Monelli et al. (2016);(7) Cusano et al. (2013); (8) Cusano et al. (2015);

(9) This work

reduction. Facility: LBT

REFERENCES

Bailey, S. I. 1902, Annals of Harvard College Observatory, 38, 1

Bressan, A., Marigo, P., Girardi, et al. 2012, MNRAS, 427, 127

Brown, T. M., Ferguson, H. C., Smith, E., et al. 2004, AJ, 127, 2738

Bullock, J. S., & Johnston, K. V. 2005, ApJ, 635, 931

Cardelli, J. A., Clayton, G. C., Mathis, J. S.1989, ApJ, 345, 245

Catelan, M. 2009, Ap& SS, 320, 261

Clement, C. M., & Rowe, J. 2000, AJ, 120, 2579

Clementini, G., Di Tomaso, S., Di Fabrizio, L., et al. 2000, AJ, 120, 2054

Clementini, G., Gratton, R., Bragaglia, et al. 2003, AJ, 125,1309

Collins, M. L. M., Chapman, S. C., Rich, R. M., et al. 2013, ApJ, 768, 172

Collins, M. L. M., Chapman, S. C., Rich, R. M., et al. 2014, ApJ, 783, 7

Conn, A. R., Ibata, R. A., Lewis, G. F., et al. 2012, ApJ, 758, 11

Crnojević, D., Sand, D. J., Zaritsky, D., et al. 2016, ApJ, 824L, 14

Cusano, F., Clementini, G., Garofalo, A., et al. 2013, ApJ, 779, 7

Cusano, F., Garofalo, A., Clementini, G., et al. 2015, ApJ, 806, 200

di Tullio, G. A. 1979, A&AS, 37, 591

Galleti, S., Federici, L., Bellazzini, M., Fusi Pecci, F., & Macrina, S. 2004, A&A, 416, 917

Gratton, R. G., Bragaglia, A., Clementini, G., et al. 2004, A&A, 421, 937

Huxor, A. P., Ferguson, A. M. N., Tanvir, N. R., et al. 2011, MNRAS, 414, 770

Ibata, R. A., Lewis, G. F., Conn, A. R., et al. 2013, Nature, 493, 62

Jacyszyn-Dobrzeniecka, A. M., Skowron, D. M., Mróz, P., et al. 2016, arXiv:1602.09141

Johnston, K. V., Choi, P. I., & Guhathakurta, P. 2002, AJ, 124, 127

Marconi, M., Fiorentino, G., & Caputo, F. 2004, A&A, 417, 1101

Martin, N. F., Ibata, R. A., McConnachie, A. W., et al. 2013, ApJ, 776, 80

McGaugh, S., & Milgrom, M. 2013, ApJ, 775, 139

Monaco, L., Bellazzini, M., Ferraro, F. R., Pancino, E. 2005, MNRAS, 356, 1396

Monelli, M., Martnez-Vzquez, C. E., Bernard, E. J. et al. 2016, ApJ, 819, 147

Oosterhoff, P. T. 1939, The Observatory, 62, 104

Pawlowski, M. S., Kroupa, P., Jerjen, H., et al. 2013, MNRAS, 435, 1928

Piersimoni, A. M., Bono, G., & Ripepi, V. 2002, AJ, 124, 1528

Pritzl, B. J., Armandroff, T. E., Jacoby, G. H., & Da Costa, G. S. 2002, AJ, 124, 1464

Pritzl, B. J., Armandroff, T. E., Jacoby, G. H., & Da Costa, G. S. 2004, AJ, 127, 318

Pritzl, B. J., Armandroff, T. E., Jacoby, G. H., & Da Costa, G. S. 2005, AJ, 129, 2232

Richardson, J. C., Irwin, M. J., McConnachie, A. W., et al. 2011, ApJ, 732, 76

Ripepi, V., Marconi, M., Moretti, M. I., et al. 2014, MNRAS, 437, 2307

Sarajedini, A., Mancone, C. L., Lauer, T. R., et al. 2009, AJ, 138, 184

Schlegel, D. J., Finkbeiner, D. P., & Davis, M. 1998, ApJ, 500, 525

Stetson, P. B. 1987, PASP, 99, 191

Stetson, P. B. 1994, PASP, 106, 250

Yang, S.-C. & Sarajedini, A. 2012,MNRAS, 419, 1362

Zaritsky, D., Crnojević, D., & Sand, D. J. 2016, arXiv:1604.08594

This 2-column preprint was prepared with the AAS LaTeX macros v5.2.